BJP British Journal of Pharmacology

DOI:10.1111/bph.12637
www.brjpharmacol.org

RESEARCH PAPER

Mitigation of carbon tetrachloride-induced hepatic injury by methylene blue, a repurposed drug, is mediated by dual inhibition of GSK3β downstream of PKA

Hong Min Wu[1], Chan Gyu Lee[1], Se Jin Hwang[2] and Sang Geon Kim[1]

[1]*College of Pharmacy and Research Institute of Pharmaceutical Sciences, Seoul National University, Seoul, Korea, and* [2]*College of Medicine, Hanyang University, Seoul, Korea*

Correspondence
Sang Geon Kim, College of Pharmacy, Seoul National University, Daehak-dong, Gwanak-gu, Seoul 151-742, Korea. E-mail: sgk@snu.ac.kr

Keywords
methylene blue; PKA; LKB1; AMPK; GSK3β

Received
11 July 2013
Revised
25 November 2013
Accepted
18 January 2014

BACKGROUND AND PURPOSE

Methylene blue (MB) has recently been considered for new therapeutic applications. In this study, we investigated whether MB has antioxidant and mitochondria-protecting effects and can prevent the development of toxicant-induced hepatitis. In addition, we explored the underlying basis of its effects.

EXPERIMENTAL APPROACH

Blood biochemistry and histopathology were assessed in mice injected with CCl_4 (0.5 mL·kg^{-1}) following MB administration (3 mg·kg^{-1}·day^{-1}, 3 days). Immunoblottings were performed to measure protein levels. Cell survival, H_2O_2, and mitochondrial superoxide and membrane permeability transition were determined in HepG2 cells.

KEY RESULTS

MB protected cells from oxidative stress induced by arachidonic acid plus iron; it restored GSH content and decreased the production of H_2O_2. It consistently attenuated mitochondria dysfunction, as indicated by inhibition of superoxide production and mitochondrial permeability transition. MB inhibited glycogen synthase kinase-3β (GSK3β) and protected the liver against CCl_4. Using siRNA, the inhibition of GSK3β was shown to depend on AMPK. MB increased the activation of AMPK *in vitro* (3–24 h) and *in vivo*. MB also increased the phosphorylation of liver kinase B1 (LKB1) via cAMP-dependent PKA. SiRNA knockdown of LKB1 eliminated phosphorylation of AMPK and inhibited MB activation of AMPK. In addition, MB treatment (≤1 h) facilitated PKA-mediated GSK3β serine phosphorylation independently of AMPK.

CONCLUSIONS AND IMPLICATIONS

MB has antioxidant and mitochondria-protecting effects and protects the liver from toxicants, which results from the dual inhibition of GSK3β by AMPK downstream of PKA-activated LKB1, and PKA itself. Our findings reveal a novel pharmacological effect of MB and its molecular basis.

Abbreviations

AA, arachidonic acid; ACC, acetyl-CoA carboxylase; ALT, alanine aminotransferase; AST, aspartate aminotransferase; CaMKKβ, calcium/calmodulin-dependent kinase kinase β; DCFH-DA, 2′,7′-dichlorofluorescein diacetate; ETC, electron transfer chain; GSK3β, glycogen synthase kinase-3β; H&E staining, haematoxylin & eosin staining; LKB1, liver kinase B1; MB, methylene blue; MMP, mitochondrial membrane potential; mPTP, mitochondrial permeability transition pore; MTT, 3-(4,5-dimethyl thiazol-2-yl)-2,5-diphenyl-tetrazolium bromide; PYK2, proline-rich tyrosine kinase 2; Rh123, rhodamine 123; ROS, reactive oxygen species; TTFA, theonyl trifluoroacetone; VDAC, voltage-dependent anion channel

Introduction

Reactive oxygen species (ROS)-induced mitochondrial dysfunction may be a critical event during the process of liver injury because it drives metabolic dysfunction, hepatocyte apoptosis, necrosis and inflammatory responses (Zorov *et al.*, 2000). A dysfunction of the electron transfer chain (ETC) complexes induces mitochondrial ROS production and this is associated with cardiovascular diseases (Suematsu *et al.*, 2003). Hence, using antioxidants to provide mitochondrial protection may have the advantage of preventing cell injury induced by toxicants, and could be therapeutic for acute or chronic diseases that are associated with cell death.

Methylene blue (MB) has now been found to have widespread biological effects and has recently become the subject of clinical investigation. For example, it is thought to have potential as a treatment for chronic degenerative illnesses (Oz *et al.*, 2009). MB can easily pass through the cell membrane and locate in the mitochondria (Gabrielli *et al.*, 2004); it keeps cycling between the reduced leucomethylene blue (MBH_2) and the oxidized (MB) form (Schirmer *et al.*, 2011; Figure 1A). During this cycling process, MB integrates leaked electrons from the mitochondrial electron transport, which helps prevent the formation of mitochondrial ROS, and increases the overall function of mitochondria (Atamna *et al.*, 2008). The most well-described effect of MB on mitochondria is associated with the ETC (i.e. alterations in ETC I-III activity, cytochrome oxidase activity and ATP restoration) (Legault *et al.*, 2011; Wen *et al.*, 2011; Daudt *et al.*, 2012). By improving mitochondrial function, MB also enhances the β-oxidation of long-chain fatty acids (Visarius *et al.*, 1999).

Glycogen synthase kinase-3β (GSK3β), a ubiquitously expressed kinase, is constitutively activated in resting cells and phosphorylates a number of substrates involved in embryonic development, protein synthesis, mitosis and cell proliferation (Forde and Dale, 2007). It is activated by ROS and controls mitochondrial function by regulating the opening of the mitochondrial permeability transition pore (mPTP), mediated by phosphorylation of the voltage-dependent anion channel (VDAC) or interaction with adenine nucleotide translocase (Das *et al.*, 2008). Hence, inhibition of GSK3β represents a potential way of improving mitochondrial function.

AMPK maintains the intracellular redox status, and plays a key role in regulating mitochondrial functions such as biogenesis, antioxidant enzyme expression (e.g. SOD, UCP2) and redox homeostasis (Xie *et al.*, 2008b; Tang *et al.*, 2011; Jeon *et al.*, 2012); it may also determine cellular antioxidant capacity. Liver kinase B1 (LKB1; Alexander *et al.*, 2013) is a primary upstream kinase of AMPK and affects mitochondrial biogenesis, cell growth, polarity and energy production (Alessi *et al.*, 2006; Shackelford and Shaw, 2009; Gan *et al.*, 2010). As MB acts specifically on mitochondria, its effect may be linked to the LKB1–AMPK pathway. Nevertheless, the effect of MB on the activity of enzymes involved in this pathway has not been examined. Moreover, the potential ability of MB to prevent and/or treat liver injury elicited by severe oxidative stress or toxicants has never been explored.

In the present study we determined whether MB acts as an antioxidant and protects mitochondria from the deleterious effects induced by severe oxidative stress, and whether it can prevent toxicant-induced hepatic injury. Moreover, we investigated the mechanisms involved and identified the signalling pathway(s) responsible for its mitochondria-protecting and antioxidant effects. Our results suggest that MB treatment activates the LKB1–AMPK pathway downstream of cAMP-dependent PKA, causing the inhibition of GSK3β in association with protection of the functional integrity of mitochondria. We also found that MB facilitated the PKA-mediated serine phosphorylation of GSK3β at an early stage. This dual inhibition of GSK3β by MB provides novel insights into the pharmacological basis for its antioxidant effect.

Methods

Materials

MB, arachidonic acid (AA), ferric nitrate, 3-(4,5-dimethyl thiazol-2-yl)-2,5-diphenyl-tetrazolium bromide (MTT), 2′,7′-dichlorofluorescein diacetate (DCFH-DA), rhodamine 123 (Rh123), rotenone, theonyl trifluoroacetone (TTFA), antimycin, KCN and anti-actin antibody were purchased from Sigma (St. Louis, MO, USA). Oligomycin, H89 and SB216763 were from Calbiochem (San Diego, CA, USA). MitoSOX was provided by Invitrogen (Carlsbad, CA, USA). Anti-PARP, anti-Bcl-xL, anti-cMyc, anti-COX2 and anti-PKA antibodies were supplied from Santa Cruz Biotechnology (Santa Cruz, CA, USA). Antibodies directed against Bcl-2, VDAC, phospho-Ser^{9}-GSK3β, GSK3β, phospho-AMPK, AMPK, acetyl-CoA carboxylase (ACC), phospho-ACC, phospho-LKB1, LKB1 and phospho-PKCζ were obtained from Cell Signaling (Beverly, MA, USA). Anti-phospho-Tyr^{216}-GSK3β and anti-iNOS antibodies were supplied by BD Biosciences (San Jose, CA, USA). The solution of iron-NTA complex was prepared as described previously (Shin *et al.*, 2009).

Cell culture

HepG2 and HeLa cells purchased from ATCC (Manassas, VA, USA) were plated in a six-well dish at a density of 1×10^6 cells per well, and wells with 70–80% confluency were used. The HepG2 cell line was used in most assays, whereas HeLa cells were used as a LKB1-deficient cell line. For cell-based experiments, MB was dissolved in sterile water (vehicle control).

MTT assay

Cell viability was assessed by MTT assays as described previously (Shin *et al.*, 2009). To measure cytotoxicity, HepG2 cells were plated at a density of 2×10^4 cells per well in a 48-well plate. After treatment, viable cells were stained with MTT (0.25 mg·mL^{-1}, 0.25–1 h). The media were then removed, and formazan crystals produced in the wells were dissolved by the addition of 200 μL DMSO. Absorbance at 540 nm was measured using an enzyme-linked immunosorbent assay microplate reader (Tecan, Research Triangle Park, NC, USA). Cell viability was defined relative to untreated control [i.e. viability (% control) = 100 × (absorbance of treated sample)/(absorbance of control)].

Determination of GSH content

Reduced GSH content was quantified using a commercial GSH determination kit (Oxis International, Portland, OR, USA). Briefly, the GSH-400 method was based on a chemical

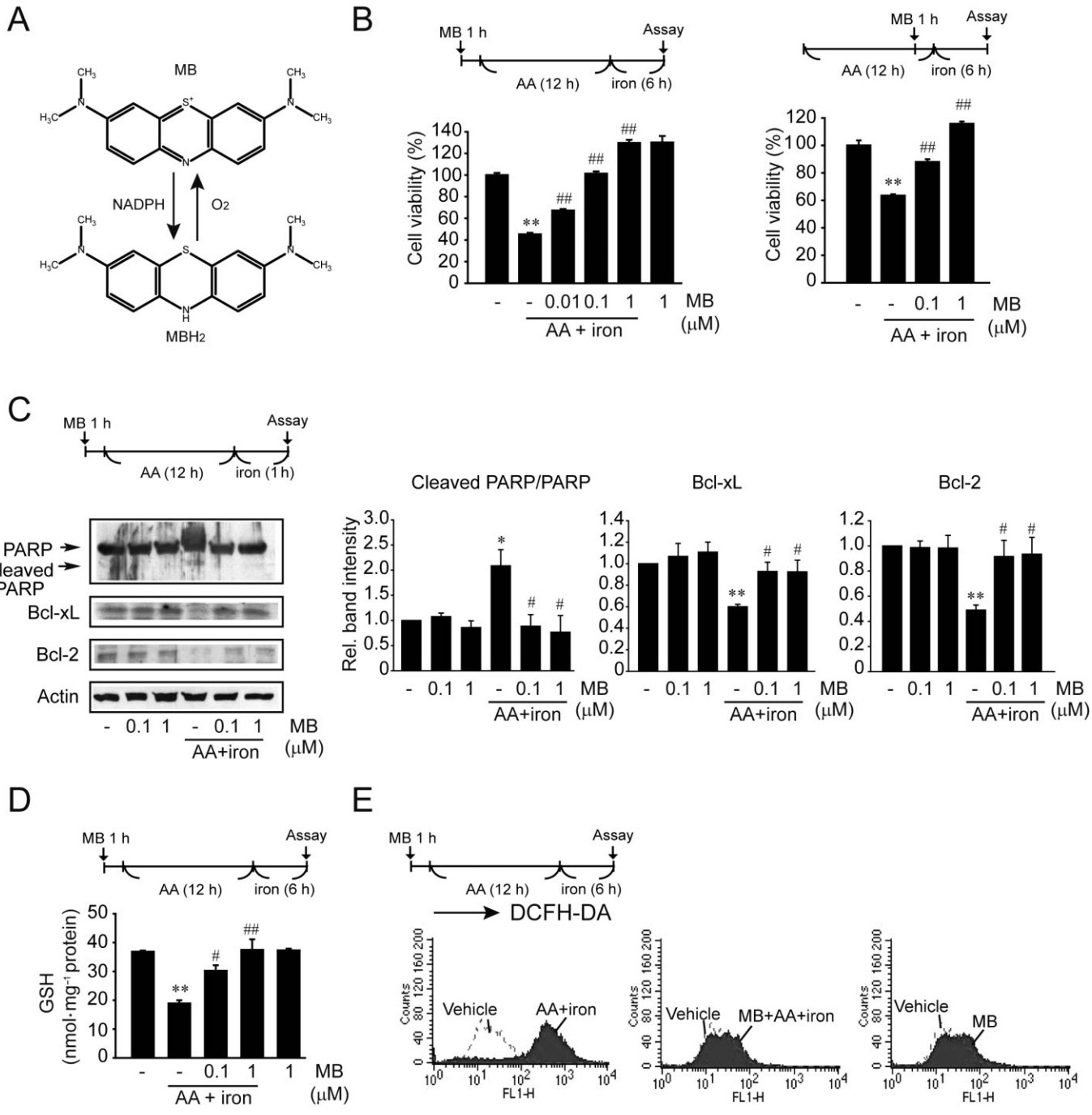

Figure 1

Increase in cell survival by MB against severe oxidative stress. (A) The chemical structures of MB and MBH_2. (B) MTT assays. HepG2 cells were treated with 0.1–1 μM MB for 1 h, and were continuously incubated with 10 μM AA for 12 h, followed by exposure to 5 μM iron for 6 h (left). The cells were also treated with MB 1 h before iron exposure in a similar way (right). Data represent the mean ± SEM of three replicates. (C) Immunoblottings. Immunoblottings were done on the cell lysates. Equal protein loading was verified by actin immunoblotting. Data represent the mean ± SEM of three separate experiments. (D) Intracellular GSH content. Data represent the mean ± SEM of three separate experiments. (E) H_2O_2 production. For (B–D), the statistical significance of differences among groups was determined (*$P < 0.05$ or **$P < 0.01$, AA + iron vs. control; and $^{\#}P < 0.05$ or $^{\#\#}P < 0.01$, AA + iron + MB vs. AA + iron).

reaction that proceeded in two steps. The first step led to the formation of thioethers between 4-chloro-1-methyl-7-trifluromethyl-quinolinum methylsulfate and all mercaptans present in the samples. The second step included β-elimination reaction under an alkaline condition. This reaction was mediated by 30% NaOH, which specifically transformed the substituted product (GSH-thioether) into a chromophoric thione (maximal absorbance wavelength = 400 nm).

Measurement of H_2O_2 production

H_2O_2 production was measured with DCFH-DA. Details are given in Supporting Information.

Measurement of mitochondrial ROS

Mitochondrial ROS production was measured with MitoSOX, as described in Supporting Information.

Flow cytometric analysis of mitochondrial membrane potential (MMP)

MMP was determined using Rh123. Details are provided in Supporting Information.

Animal treatments

Animal studies were conducted in accordance with the institutional guidelines for care and use of laboratory animals, and were approved by the Institutional Animal Care and Use Committee (IACUC), Seoul National University. All studies involving animals are reported in accordance with the ARRIVE guidelines for reporting experiments involving animals (Kilkenny *et al.*, 2010; McGrath *et al.*, 2010). A total of 16 male C57BL mice (6 weeks old) supplied from Charles River Orient (Seoul, Korea) were used in the experiments described here. The mice were caged and acclimatized for 1 week in a clean room at the Animal Centre for Pharmaceutical Research, Seoul National University, and were supplied with filtered air, commercial chow (Purina, Korea) and water *ad libi*tum at a temperature between 20 and 23°C with a 12 h light and dark cycle and relative humidity of 50%. MB was dissolved in tap water (vehicle control) and was administered p.o. to mice (n = 4) at a dose of 3 $mg \cdot kg^{-1} \cdot day^{-1}$ for 3 consecutive days. At 6 h after the last dose of MB (on day 3), the mice were injected with CCl_4 (i.p., 0.5 $mL \cdot kg^{-1}$ body wt, 1:20 in corn oil). All mice were killed 48 h after the CCl_4 injection.

Haematoxylin & eosin staining (H&E) or oil red O staining

H&E staining and oil red O staining were done as described in Supporting Information.

Blood biochemical analysis

Alanine aminotransferase (ALT), aspartate aminotransferase (AST) activities, TNFα or IL-1β contents in plasma were measured as described in Supporting Information.

Immunoblot analysis

Immunoblot analyses were performed as described in Supporting Information.

siRNA knockdown

Cells were transfected with either a siRNA directed against human PKA or LKB1 (Santa Cruz, CA, USA), or a non-targeting control siRNA (100 nM) using AMAXA nucleofection system (Lonza, Köln, Germany). Immunoblottings verified the knockdown effect of PKA or LKB1.

Plasmid transfection

Cells were transfected with the plasmid encoding for cMyc-tagged DN-AMPK (provided by Dr J. Ha, Kyung Hee University, Korea) or pCDNA3.1 (1 μg) using FuGENE® reagent (Roche, Nutley, NJ, USA) for 24 h.

Data analysis

Data represent the mean ± SEM and were compared among groups using one-way ANOVA and/or analysed using Student's t test. $P < 0.05$ was considered to be statistically significant.

Results

Inhibition of cell injury against severe oxidative stress

To determine whether MB treatment protects cells from injury induced by oxidative stress, we first used an *in vitro* cell injury model (Shin *et al.*, 2009). MB treatment before the addition of AA + iron completely protected HepG2 cells from severe oxidative stress (Figure 1B, left). To assess the effect of MB at an early time, viability was measured in the cells treated with MB 1 h before the addition of iron (Figure 1B, right); cell viability was also entirely retained in this experiment. The cytoprotective effect of MB was verified by changes in the levels of apoptotic (e.g. cleaved PARP) or anti-apoptotic markers (e.g. Bcl-xL and Bcl-2) (Figure 1C). In addition, MB treatment enabled cells to retain their GSH content when challenged with AA + iron (Figure 1D). The increased H_2O_2 production induced by AA + iron was also attenuated by MB (Figure 1E). These results show that MB exerts a cytoprotective and antioxidant effect against severe oxidative stress.

Protection of mitochondrial integrity

Next, we examined the effect of MB on the formation of mitochondrial superoxide using MitoSOX. Treatment with AA + iron caused a rightward shift of MitoSOX fluorescence, indicating increased production of mitochondrial ROS, which was abolished by MB treatment (Figure 2A). In the assays using Rh123 (a sensitive probe of MMP), MB prevented the increase in the number of Rh123-negative cells (i.e. M1 fraction represents mitochondrial dysfunction) (Figure 2B). Similarly, the oligomerization of VDAC (e.g. trimerization and tetramerization) was decreased by MB (Figure 2C) (Keinan *et al.*, 2010). Inhibitors of mitochondrial complexes that are specific for each complex cause ROS production and apoptosis (Mills *et al.*, 1996; Chen *et al.*, 2007; Tettamanti *et al.*, 2008; Xu *et al.*, 2013). So, we sought to determine whether MB treatment protects mitochondria against the

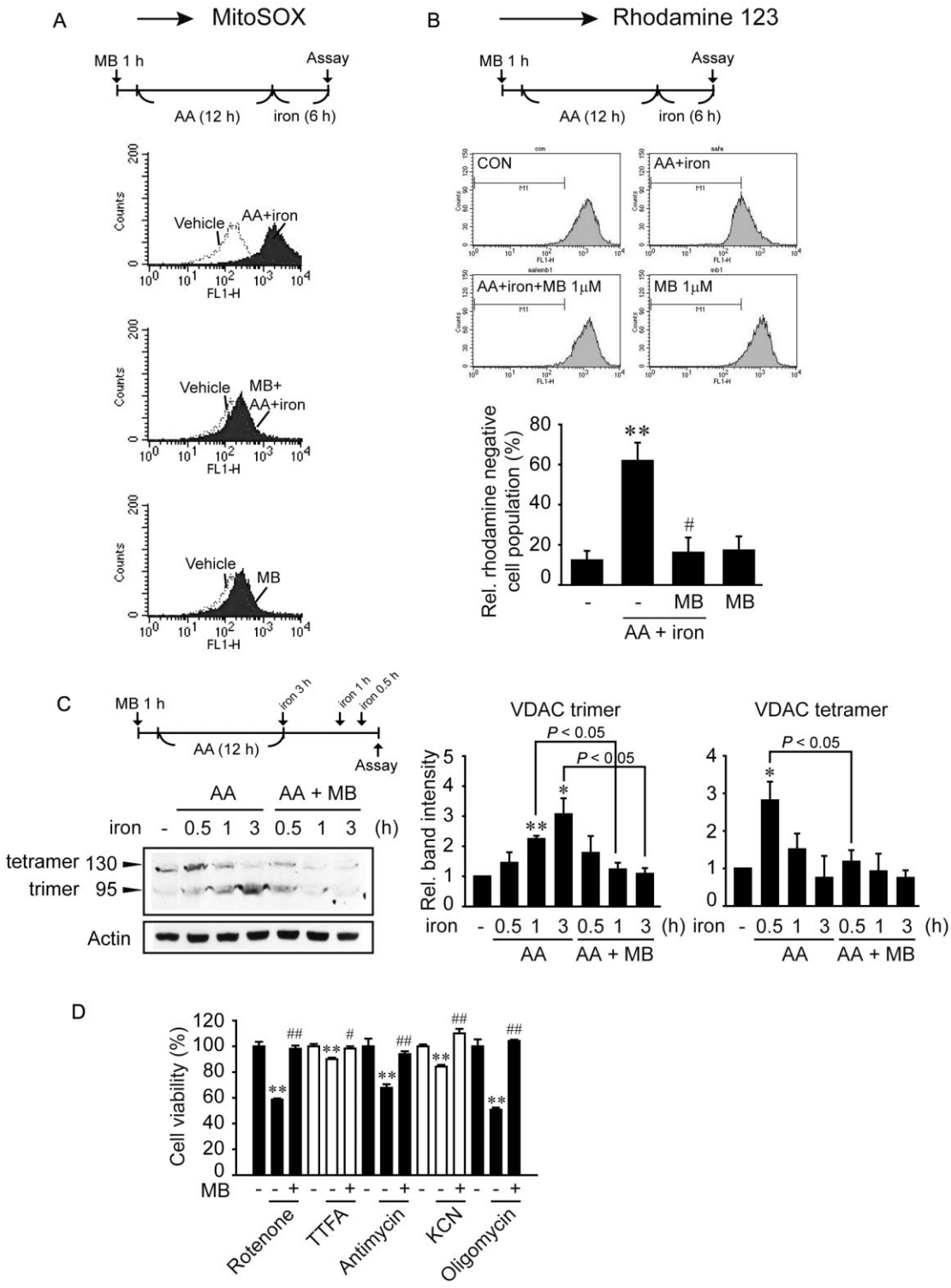

Figure 2

MB protects mitochondria from the effects of severe oxidative stress. (A) Mitochondrial superoxide production. Superoxide was monitored using MitoSOX assays in HepG2 cells treated as described in Figure 1B left. (B) Mitochondrial membrane permeability transition. The percentage of cells in the M1 fraction was quantified. Data represent the mean ± SEM of three separate experiments (**$P < 0.01$, AA + iron vs. control; and $^{\#}P < 0.05$, AA + iron + MB vs. AA + iron). (C) VDAC oligomerization. HepG2 cells were treated with 1 μM MB for 1 h, and were continuously incubated with 10 μM AA for 12 h, followed by exposure to 5 μM iron for 0.5–3 h. Immunoblotting for VDAC was done on cell lysates. Data represent the mean ± SEM of three separate experiments (*$P < 0.05$ or **$P < 0.01$, AA + iron vs. control). (D) MTT assays. HepG2 cells were treated with 1 μM MB for 1 h, followed by exposure to 100 μM rotenone, 100 μM TTFA, 50 μg·mL^{-1} antimycin, 100 μM KCN or 50 μM oligomycin for 24 h. Data represent the mean ± SEM of four replicates (**$P < 0.01$, ETC inhibitor vs. control; and $^{\#}P < 0.05$ or $^{\#\#}P < 0.01$, ETC inhibitor + MB vs. ETC inhibitor).

effects of mitochondrial complex inhibitors (Figure 2D). The viability of cells was fully or significantly protected by MB from the effects of rotenone (complex I inhibitor), TTFA (complex II inhibitor), antimycin (complex III inhibitor), KCN (complex IV inhibitor) or oligomycin (complex V inhibitor), indicating that MB enhances mitochondrial respiratory activity. All of these results show that MB has the ability to protect mitochondria from the effects of oxidative stress and/or enhances mitochondrial respiratory function.

Increase in GSK3β serine phosphorylation

Inhibition of GSK3β protects mitochondria from ischaemic/reperfusion injury (Park *et al.*, 2006). Next, we determined whether MB has an inhibitory effect on GSK3β in association with its mitochondria-protective effect. MB treatment facilitated the inhibitory serine phosphorylation of GSK3β but repressed its tyrosine phosphorylation (activating) in a time-dependent manner (Figure 3A, upper). Consequently, the ratio of its tyrosine : serine phosphorylation began to markedly decrease as early as 30 min after MB treatment, and remained decreased for, at least, up to 24 h (Figure 3A, lower). In primary rat hepatocytes, MB had a similar effect (Supporting Information Figure S1). The functional role of GSK3β inhibition in protecting mitochondria from oxidative stress was confirmed by the retention of cell viability after treatment with SB216763, a known GSK3β inhibitor (Figure 3B).

Inhibition of liver injury against CCl_4 treatment

We next tested the hepatoprotective effect of MB in a mouse model. MB treatment notably decreased CCl_4-induced hepatic injury and steatosis, as shown by liver H&E staining or oil red O staining (Figure 4A and B). The results of blood biochemistry confirmed this liver-protective effect: plasma ALT and AST activities were elevated 48 h after a single dose of CCl_4, and these effects were prevented by MB treatment (Figure 4C). CCl_4 treatment increased tyrosine phosphorylation of GSK3β (Figure 4D). In addition, its serine phosphorylation was unexpectedly elevated presumably due to an adaptive response to the toxicant. MB treatment decreased both tyrosine- and serine-phosphorylated GSK3β levels (Figure 4D). Our data showing a significant decrease in the ratio of tyrosine : serine phosphorylation of GSK3β indicate that MB reduces the net activity of GSK3β. These results show that the ability of MB to protect the liver from the CCl_4 insult is associated with GSK3β inhibition.

AMPK activation

AMPK activation leads to the inhibition of GSK3β and protects mitochondria (Choi *et al.*, 2010). Given the link between AMPK and GSK3β, we assessed whether MB facilitates AMPK activation. Treatment of HepG2 cells with MB enhanced phospho-AMPK levels in a time-dependent manner (3–24 h) (Figure 5A). A similar outcome was obtained in primary rat hepatocytes (Supporting Information

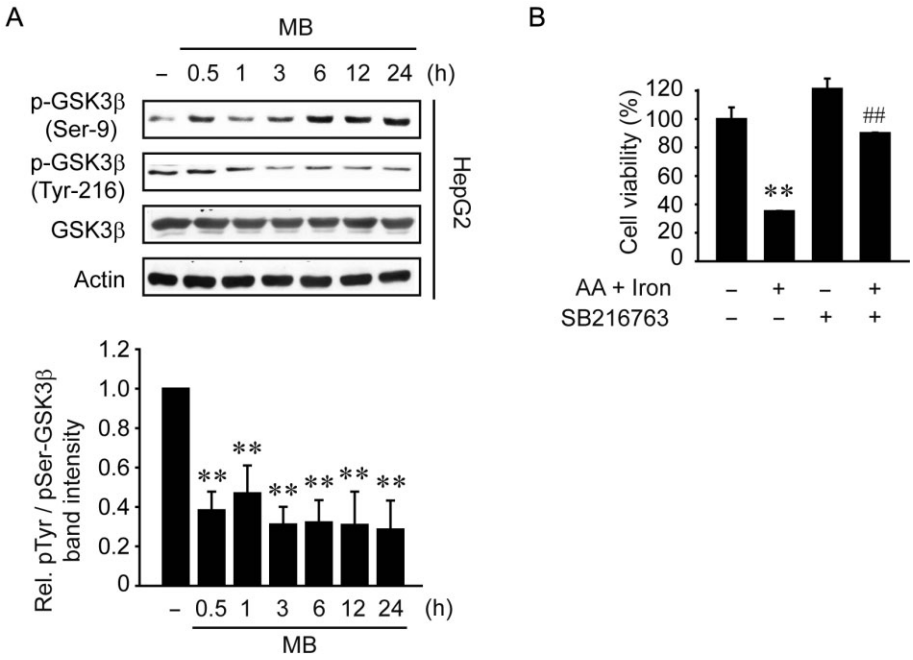

Figure 3

The effect of MB on GSK3β serine or tyrosine phosphorylation. (A) Immunoblottings for phosphorylated GSK3β. Immunoblottings were done on the lysates of HepG2 cells treated with 1 μM MB for the indicated times. Data represent the mean ± SEM of four separate experiments (**$P < 0.01$, MB vs. control). (B) MTT assays. HepG2 cells were treated with 10 μM SB216763 for 1 h, and continuously incubated with 10 μM AA for 12 h, followed by exposure to 5 μM iron for 6 h. Data represent the mean ± SEM of three replicates (**$P < 0.01$, AA + iron vs. control; and $^{\#\#}P < 0.01$, AA + iron + SB216763 vs. AA + iron).

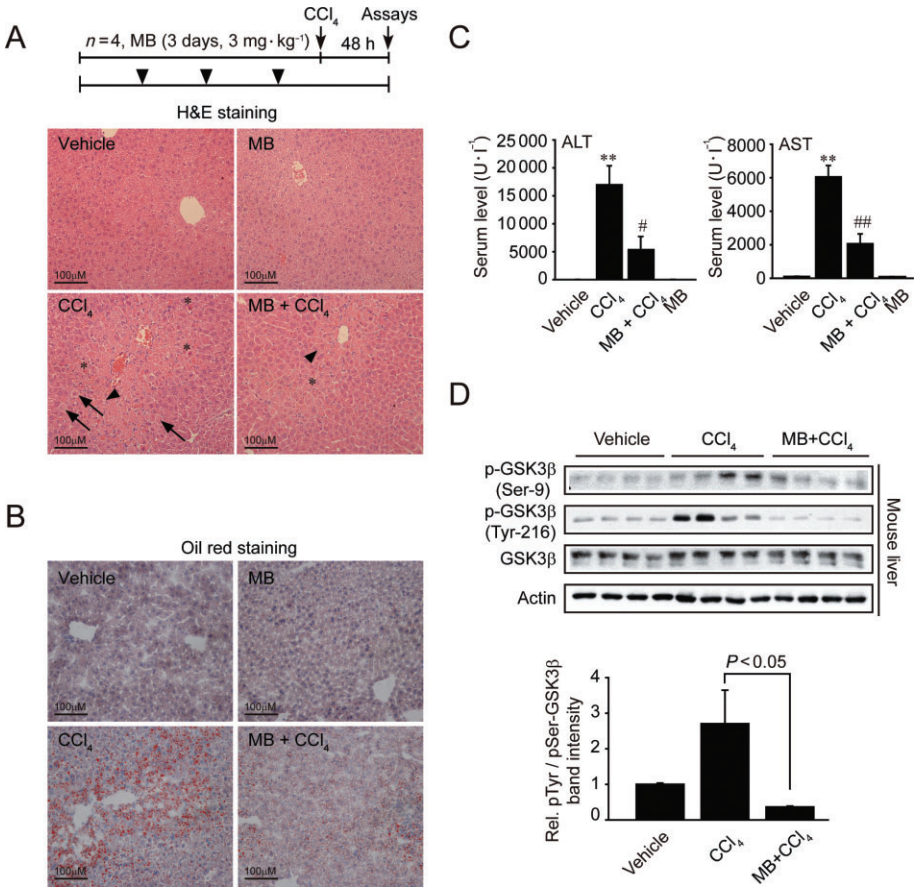

Figure 4

The liver-protective effect of MB against CCl_4. (A) H&E staining of the liver sections. MB was administered p.o. to mice (n = 4) at a dose of 3 mg·kg^{-1}·day^{-1} for 3 consecutive days. At 6 h after the last dose of MB, mice were injected with CCl_4 (i.p., 0.5 mL·kg^{-1} body wt, 1:20 in corn oil) and killed 48 h thereafter. The representative pictures show liver H&E staining (original magnification 200×). Asterisks indicate eosinophilic necrosis of hepatocytes. Arrowheads show lipid droplets, whereas arrows indicate hepatocyte swelling. (B) Oil red O staining. The representative pictures show oil red O staining of liver sections (original magnification 200×). (C) Plasma ALT and AST activities. Data represent the mean ± SEM of four animals (**$P < 0.01$, CCl_4 vs. vehicle; and $^{\#}P < 0.05$ or $^{\#\#}P < 0.01$, CCl_4 + MB vs. CCl_4). (D) The levels of Ser^{9}- or Tyr^{216}-phosphorylated GSK3β in the liver.

Figure S1). Consistently, the phosphorylation of ACC, a representative substrate of AMPK, was augmented. AMPK phosphorylation was also enhanced in the liver of mice treated with MB alone (Figure 5B). These results provide evidence that MB activates AMPK both *in vitro* and *in vivo*.

LKB1 phosphorylation

We then tested whether MB affects LKB1, an upstream kinase of AMPK. In HepG2 cells, the phosphorylation of LKB1 was notably increased 1–24 h after MB treatment (Figure 6A). Similar changes were found in primary hepatocytes (Supporting Information Figure S1). As expected, siRNA knockdown of LKB1 eliminated the phosphorylation of AMPK (Figure 6B, left). In LKB1-deficient HeLa cells, MB did not activate AMPK (Figure 6B, middle). In addition to LKB1, calcium/calmodulin-dependent kinase kinase β (CaMKKβ) is another upstream kinase of AMPK (Hurley *et al.*, 2005). Treatment of HepG2 cells with STO-609 (0.3–3 μg·mL^{-1}), an inhibitor CaMKKβ, failed to antagonize AMPK activation by MB (Figure 6B, right; Supporting Information Figure S2). Our results, therefore, demonstrate that MB activates AMPK through LKB1, but not through CaMKKβ.

PKA-dependent phosphorylation of LKB1 and GSK3β

In an effort to find the upstream kinase of LKB1, we determined whether LKB1 phosphorylation by MB relies on PKA, because PKA may activate LKB1 via phosphorylation (Collins *et al.*, 2000). In this assay, a 1 h time point was included as an indicator of the early response because GSK3β phosphorylation occurred as early as 30 min after MB treatment, whereas significant increases in the phosphorylation of LKB1 and AMPK were observed beginning from 1 h and 6 h respectively. So, we presumed that the phosphorylation of GSK3β at 1 h reflected an early response. A deficiency in PKA entirely inhibited the ability of MB to phosphorylate LKB1 throughout the time points examined (1–12 h) (Figure 7A), indicating that PKA is required for the activation of LKB1. The levels of

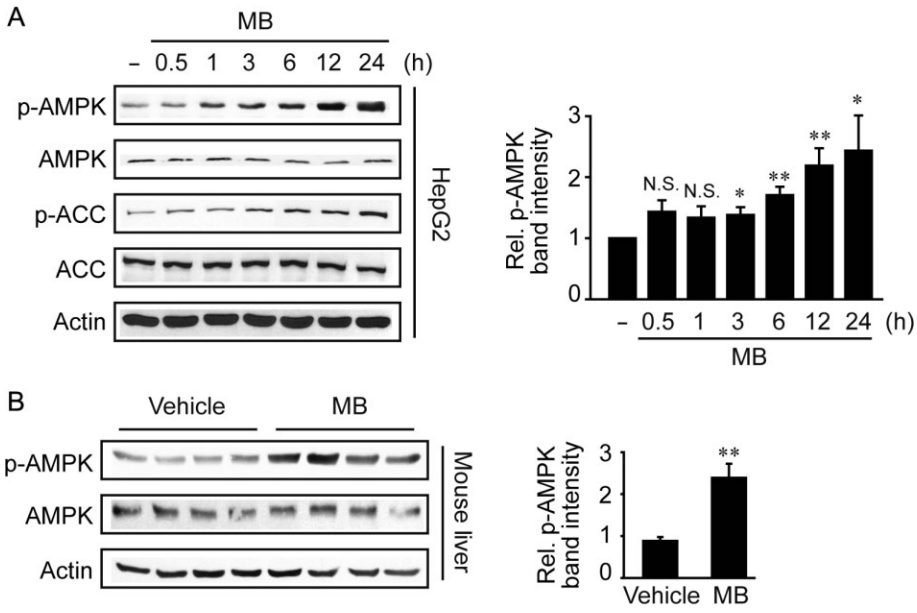

Figure 5

AMPK activation by MB. (A) AMPK activation *in vitro*. Immunoblottings were done on the lysates of HepG2 cells treated with 1 μM MB for the indicated times. Data represent the mean ± SEM of four separate experiments (*$P < 0.05$ or **$P < 0.01$, MB vs. control). N.S., not significant. (B) AMPK activation *in vivo*. Immunoblottings were done on the liver samples obtained from mice treated with vehicle or MB alone, as described in Figure 4A. Data represent the mean ± SEM of four animals (**$P < 0.01$, MB vs. vehicle).

phosphorylated PKCζ, another kinase that activates LKB1 (Xie *et al.*, 2008a), were not enhanced by MB (Figure 7B), further corroborating the role of PKA in the activation of LKB1.

Having identified the role of PKA in activating the LKB1–AMPK pathway, we next evaluated the role of AMPK in the phosphorylation of GSK3β at the early and late times (i.e. 1 h vs. 12 h). Of note, DN-AMPK transfection did not antagonize the ability of MB to increase GSK3β phosphorylation at 1 h, whereas it did so at 12 h (Figure 7C). Our data raised the possibility that the phosphorylation of GSK3β observed at the early time (i.e. 30 min–1 h) after MB treatment is not mediated by AMPK, although it depends on AMPK thereafter. Consistently, PKA inhibition using siRNA or H89 (an inhibitor of PKA) completely prevented the increase in GSK3β serine phosphorylation 1 h after MB treatment (Figure 7D). Collectively, it is highly likely that PKA phosphorylates GSK3β at serine at an early time (i.e. ≤1 h), whereas AMPK activated by LKB1 downstream from PKA leads to the phosphorylation of GSK3β thereafter at least up to 24 h.

Discussion and conclusions

Antioxidants may serve as potential therapeutic agents for various diseases. The effects of several antioxidants have been tested in patients with liver diseases (Bjelakovic *et al.*, 2011). However, only some of them have shown promising results in observational and clinical trials. So there is a need to discover new drugs with improved activity and low cost. MB has recently been further investigated, as a repurposed drug, for new therapeutic uses (Devine *et al.*, 1983; Preiser *et al.*, 1995; Link, 1999; Rodrigues *et al.*, 2007). Our results shown here revealed that MB has a *bona fide* antioxidant effect both *in vitro* and *in vivo*: (i) a cell model exposed to severe oxidative stress; and (ii) an animal model with acute toxicant-induced hepatitis.

Overproduction of mitochondrial ROS and the consequent formation of mPTP may lead to the incomplete reduction of oxygen at several sites on the ETC. Here, we showed that MB treatment prevented mitochondrial superoxide formation elicited by AA + iron, maintaining the integrity and function of mitochondria. This was substantiated by the inhibition of oligomerization of VDAC that mediates mPTP formation and apoptotic cytochrome *c* release (Keinan *et al.*, 2010). MB is reduced by NADPH or thioredoxin to become MBH_2, which can then be re-oxidized by O_2; this cycling process enables it to interact with mitochondria (Gabrielli *et al.*, 2004; Schirmer *et al.*, 2011). So, MB may enhance ATP restoration in mitochondria (Legault *et al.*, 2011). Our finding that MB treatment protected cells from the deleterious effects of all of the inhibitors that intervene with each of mitochondrial complexes agrees with this idea.

GSK3β-mediated mPTP opening accounts for the progression of diseases resulting from mitochondrial dysfunction. Hence, inhibition of GSK3β represents a potential way to improve mitochondrial function (Petit-Paitel *et al.*, 2009); Ser^9 phosphorylation of GSK3β contributes to cell survival by modulating mPTP opening (Park *et al.*, 2006). GSK3β activity is increased by phosphorylation at Tyr^{216} or dephosphorylation at Ser^9. An important finding of our study is the demonstration of the ability of MB to enhance the inhibitory phosphorylation of GSK3β (Ser^9). The decrease in Tyr^{216} phos-

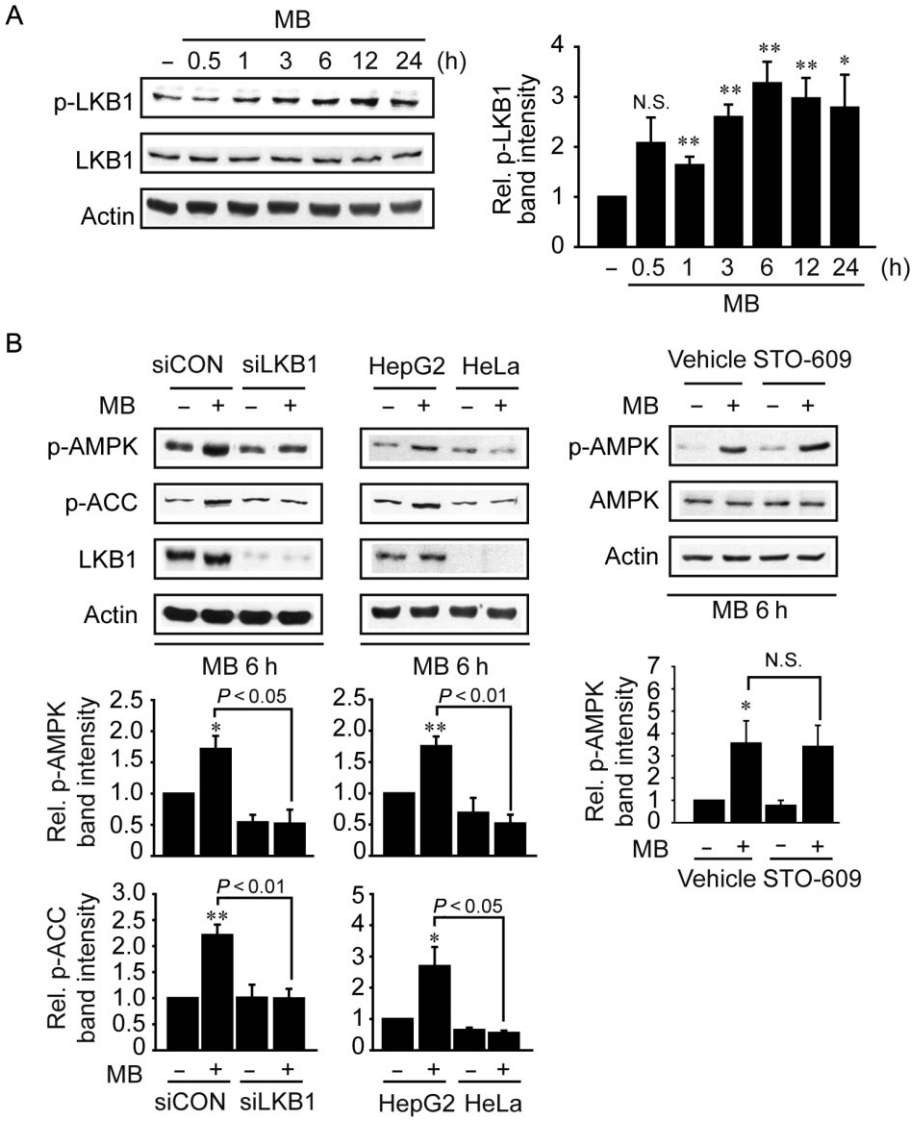

Figure 6

Activation of LKB1 by MB. (A) Immunoblottings for phosphorylated LKB1. Immunoblottings were performed on the lysates of cells treated as described in Figure 3A. Data represent the mean ± SEM of four separate experiments (*$P < 0.05$ or **$P < 0.01$, MB vs. control). N.S., not significant. (B) LKB1-dependent AMPK activation. HepG2 cells were treated with 1 μM MB for 6 h after transfection of control siRNA or siRNA directed against LKB1 (100 nM, 48 h) (left). HepG2 or HeLa cells were treated with 1 μM MB (middle). HepG2 cells were exposed to 1 μg·mL^{-1} STO-609 (CaMKKβ inhibitor) for 30 min, and continuously incubated with 1 μM MB for 6 h (right). *$P < 0.05$ or **$P < 0.01$, MB versus control.

phorylation of GSK3β along with an increase in its Ser^{9} phosphorylation supports its antioxidant capacity.

Proline-rich tyrosine kinase 2 (PYK2) has been shown to phosphorylate GSK3β at the Tyr^{216} residue (Sayas *et al.*, 2006). However, we failed to detect a decrease in PYK2 levels in MB-treated HepG2 cells (data not shown), which may be due to the low expression levels of PYK2 in an epithelial-type of cells (Sun *et al.*, 2007). In the present study, we observed an increase in Tyr^{216} phosphorylation of GSK3β in the liver of mice treated with CCl_4. Ser^{9} phosphorylation of GSK3β may also have increased as an adaptive response to the toxic insult in this animal model. Our finding that MB treatment decreased both Tyr^{216}- and Ser^{9}-phosphorylated GSK3β levels supports this possibility.

An important finding of our study is the discovery of MB's effect on AMPK activation. Our results clearly showed that MB treatment gradually promoted the phosphorylation of AMPK at least up to 24 h in hepatocytes, as also verified by the *in vivo* experiment, and this effect was shown to depend on the activation of the phosphorylation of LKB1. In fact, antioxidants including resveratrol, polyphenols and flavonoids have the ability to activate the LKB1–AMPK signalling, thereby protecting mitochondria (Shin *et al.*, 2009; Choi *et al.*, 2010; Kim *et al.*, 2012). So, the activation of the LKB1–AMPK pathway by MB is in line with its ability to increase mitochondrial capacity and cell survival.

PKA plays a key role in the regulation of energy metabolism by phosphorylating a variety of targets, and had been pro-

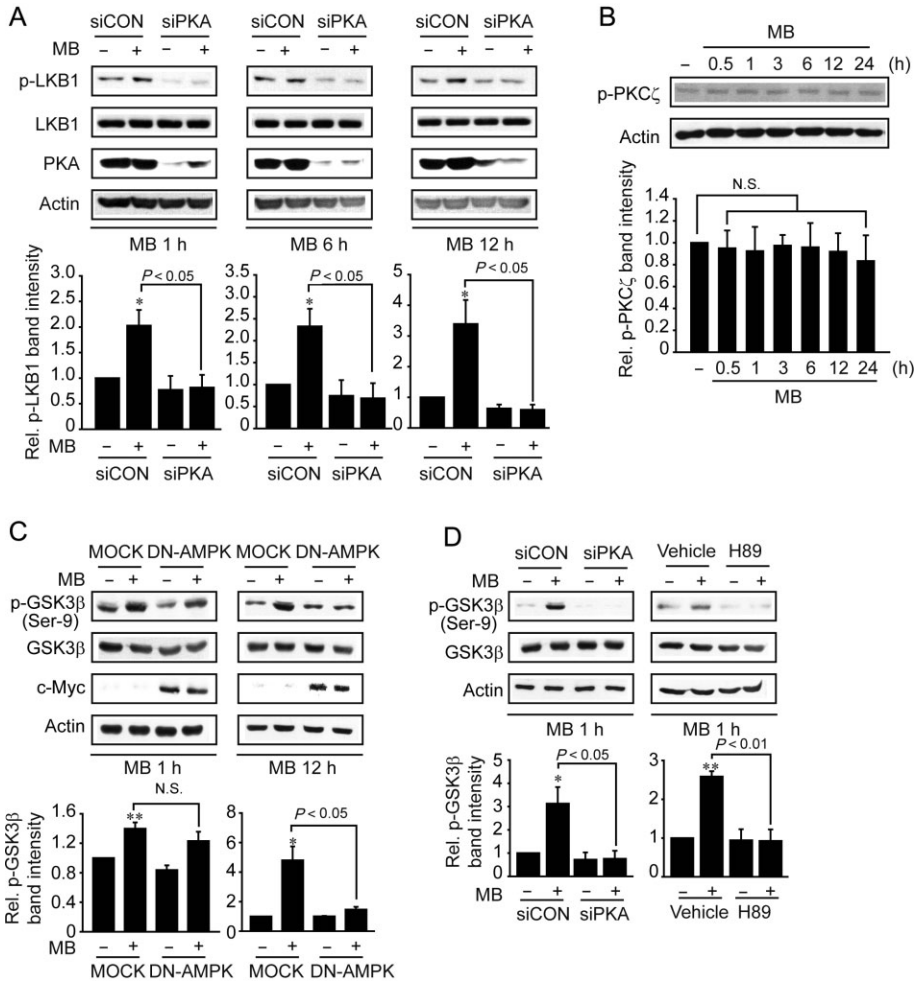

Figure 7

The role of PKA in the phosphorylation of LKB1 and GSK3β by MB. (A) The effect of PKA knockdown on the phosphorylation of LKB1. HepG2 cells were treated with 1 μM MB for the indicated times following transfection with siRNA (100 nM, 48 h). (B) Immunoblotting for phosphorylated PKCζ. Immunoblottings were done on cell lysates as described in Figure 3A. (C) The effect of DN-AMPK transfection on GSK3β serine phosphorylation. HepG2 cells were transfected with DN-AMPK and exposed to 1 μM MB for 1 or 12 h. (D) Attenuation of GSK3β serine phosphorylation by PKA inhibition. HepG2 cells were either transfected with siRNA (100 nM, 48 h) or treated with H89 (1 μM, 30 min), and were incubated with 1 μM MB for 1 h. For (A–D), data represent the mean ± SEM of three separate experiments (*$P < 0.05$ or **$P < 0.01$, MB vs. control). N.S., not significant.

posed to be involved in the regulation of ROS (Ryu *et al.*, 2005). Our result that PKA was necessary for the phosphorylation of LKB1 by MB clearly demonstrates the beneficial role of PKA in preventing ROS-mediated apoptosis. PKA phosphorylation at the threonine residue was assessed in cell-based assays, as it is a key step for its maturation and activity (Cheng *et al.*, 1998); MB was shown to prevent the reduction in the level of PKA and its phosphorylation induced by AA + iron (Supporting Information Figure S3A). Moreover, we observed a similar effect in mice treated with CCl_4 (Supporting Information Figure S3B). However, in multiple assays, we could not detect reproducible significant activation of PKA by MB (data not shown). As cAMP-dependent PKA activation is transient (e.g. 1–10 min) (Roberson and Sweatt, 1996), MB may activate PKA momentarily, if at all. PKA may be localized in subcellular organelles including mitochondria (Dagda *et al.*, 2011). In our assay, we did not observe mitochondria translocation of PKA (Supporting Information Figure S3C). Hence, the mechanism of PKA activation by MB remains to be clarified.

Another intriguing finding of our study is that PKA controlled serine phosphorylation of GSK3β by MB not only early on the experiment but also later on. It had been shown that PKA activators (8-Br-cAMP and forskolin) inhibit GSK3β at an early time (<30 min) (Fang *et al.*, 2000). However, it is not known for how long PKA inhibits GSK3β. Here, we demonstrated that PKA-mediated GSK3β inhibition by MB at the early time contributes to cell survival against the toxicant. Moreover, we found an additional effect of MB on GSK3β at the later time, but this was dependent on the activities of LKB1 and AMPK downstream of PKA, indicating the critical role of LKB1–AMPK signalling in the prolonged inhibition of GSK3β by PKA.

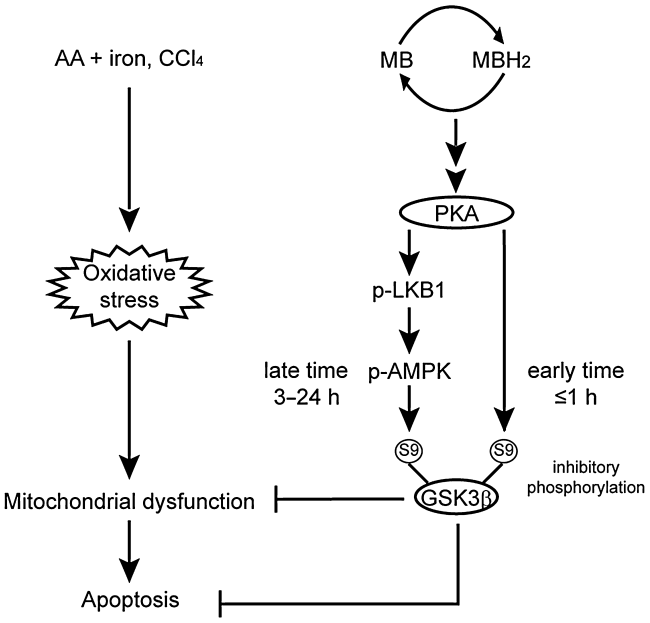

Figure 8

A schematic illustration of the proposed mechanism by which MB protects cells against oxidative injury.

In both the cell-based and animal experiments, LKB1 and AMPK phosphorylation were diminished by the toxicants, and this effect was prevented by MB (Supporting Information Figure S4). Additionally, MB had an anti-inflammatory effect, as it prevented the CCl_4-induced increased TNFα and IL-1β levels in the plasma, and iNOS and COX2 expression in the liver (Supporting Information Figure S5); MB alone slightly, but significantly, increased IL-1β, but this needs further clarification.

Taken together, our results demonstrate that MB inhibits oxidative stress-induced liver injury and hepatocyte death, and this may result from the inhibition of GSK3β, which is mediated by both PKA-dependent LKB1–AMPK activation and PKA itself (Figure 8). All of these results support the *bona fide* antioxidant effect of MB at pharmacologically active concentrations, indicating that MB may be of use for the prevention and/or treatment of acute liver injury.

Acknowledgements

This work was supported by the National Research Foundation of Korea (NRF) grant funded by the Korea government (MSIP) (No. 2007-0056817) and in part by the World Class University project (R32-2012-000-10098-0).

Conflict of interest

The authors disclose no conflicts.

References

Alessi DR, Sakamoto K, Bayascas JR (2006). LKB1-dependent signaling pathways. Annu Rev Biochem 75: 137–163.

Alexander SPH, Benson HE, Faccenda E, Pawson AJ, Sharman JL, Spedding M, Peters JA, Harmar AJ and CGTP Collaborators (2013). The Concise Guide to PHARMACOLOGY 2013/14: Enzymes. Br J Pharmacol 170: 1797–1867.

Atamna H, Nguyen A, Schultz C, Boyle K, Newberry J, Kato H *et al.* (2008). Methylene blue delays cellular senescence and enhances key mitochondrial biochemical pathways. FASEB J 22: 703–712.

Bjelakovic G, Gluud LL, Nikolova D, Bjelakovic M, Nagorni A, Gluud C (2011). Antioxidant supplements for liver diseases. Cochrane Database Syst Rev (3): CD007749.

Chen Y, McMillan-Ward E, Kong J, Israels SJ, Gibson SB (2007). Mitochondrial electron-transport-chain inhibitors of complexes I and II induce autophagic cell death mediated by reactive oxygen species. J Cell Sci 120: 4155–4166.

Cheng X, Ma Y, Moore M, Hemmings BA, Taylor SS (1998). Phosphorylation and activation of cAMP-dependent protein kinase by phosphoinositide-dependent protein kinase. Proc Natl Acad Sci U S A 95: 9849–9854.

Choi SH, Kim YW, Kim SG (2010). AMPK-mediated GSK3beta inhibition by isoliquiritigenin contributes to protecting mitochondria against iron-catalyzed oxidative stress. Biochem Pharmacol 79: 1352–1362.

Collins SP, Reoma JL, Gamm DM, Uhler MD (2000). LKB1, a novel serine/threonine protein kinase and potential tumour suppressor, is phosphorylated by cAMP-dependent protein kinase (PKA) and prenylated in vivo. Biochem J 345 (Pt 3): 673–680.

Dagda RK, Gusdon AM, Pien I, Strack S, Green S, Li C *et al.* (2011). Mitochondrially localized PKA reverses mitochondrial pathology and dysfunction in a cellular model of Parkinson's disease. Cell Death Differ 18: 1914–1923.

Das S, Wong R, Rajapakse N, Murphy E, Steenbergen C (2008). Glycogen synthase kinase 3 inhibition slows mitochondrial adenine nucleotide transport and regulates voltage-dependent anion channel phosphorylation. Circ Res 103: 983–991.

Daudt DR 3rd, Mueller B, Park YH, Wen Y, Yorio T (2012). Methylene blue protects primary rat retinal ganglion cells from cellular senescence. Invest Ophthalmol Vis Sci 53: 4657–4667.

Devine RM, van Heerden JA, Grant CS, Muir JJ (1983). The role of methylene blue infusion in the management of persistent or recurrent hyperparathyroidism. Surgery 94: 916–918.

Fang X, Yu SX, Lu Y, Bast RC Jr, Woodgett JR, Mills GB (2000). Phosphorylation and inactivation of glycogen synthase kinase 3 by protein kinase A. Proc Natl Acad Sci U S A 97: 11960–11965.

Forde JE, Dale TC (2007). Glycogen synthase kinase 3: a key regulator of cellular fate. Cell Mol Life Sci 64: 1930–1944.

Gabrielli D, Belisle E, Severino D, Kowaltowski AJ, Baptista MS (2004). Binding, aggregation and photochemical properties of methylene blue in mitochondrial suspensions. Photochem Photobiol 79: 227–232.

Gan B, Hu J, Jiang S, Liu Y, Sahin E, Zhuang L *et al.* (2010). LKB1 regulates quiescence and metabolic homeostasis of haematopoietic stem cells. Nature 468: 701–704.

Hurley RL, Anderson KA, Franzone JM, Kemp BE, Means AR, Witters LA (2005). The Ca2+/.calmodulin-dependent protein kinase kinases are AMP-activated protein kinase kinases. J Biol Chem 280: 29060–29066.

Jeon SM, Chandel NS, Hay N (2012). AMPK regulates NADPH homeostasis to promote tumour cell survival during energy stress. Nature 485: 661–665.

Keinan N, Tyomkin D, Shoshan-Barmatz V (2010). Oligomerization of the mitochondrial protein voltage-dependent anion channel is coupled to the induction of apoptosis. Mol Cell Biol 30: 5698–5709.

Kilkenny C, Browne W, Cuthill IC, Emerson M, Altman DG (2010). Animal research: Reporting *in vivo* experiments: the ARRIVE guidelines. Br J Pharmacol 160: 1577–1579.

Kim AY, Lee CG, Lee DY, Li H, Jeon R, Ryu JH *et al*. (2012). Enhanced antioxidant effect of prenylated polyphenols as Fyn inhibitor. Free Radic Biol Med 53: 1198–1208.

Legault J, Larouche PL, Côté I, Bouchard L, Pichette A, Robinson BH *et al*. (2011). Low-concentration methylene blue maintains energy production and strongly improves survival of Leigh syndrome French Canadian skin fibroblasts. J Pharm Pharm Sci 14: 438–449.

Link EM (1999). Targeting melanoma with 211At/131I-methylene blue: preclinical and clinical experience. Hybridoma 18: 77–82.

McGrath J, Drummond G, McLachlan E, Kilkenny C, Wainwright C (2010). Guidelines for reporting experiments involving animals: the ARRIVE guidelines. Br J Pharmacol 160: 1573–1576.

Mills EM, Gunasekar PG, Pavlakovic G, Isom GE (1996). Cyanide-induced apoptosis and oxidative stress in differentiated PC12 cells. J Neurochem 67: 1039–1046.

Oz M, Lorke DE, Petroianu GA (2009). Methylene blue and Alzheimer's disease. Biochem Pharmacol 78: 927–932.

Park SS, Zhao H, Mueller RA, Xu Z (2006). Bradykinin prevents reperfusion injury by targeting mitochondrial permeability transition pore through glycogen synthase kinase 3beta. J Mol Cell Cardiol 40: 708–716.

Petit-Paitel A, Brau F, Cazareth J, Chabry J (2009). Involvement of cytosolic and mitochondrial GSK-3beta in mitochondrial dysfunction and neuronal cell death of MPTP/MPP-treated neurons. PLoS ONE 4: e5491.

Preiser JC, Lejeune P, Roman A, Carlier E, De-Backer D, Leeman M *et al*. (1995). Methylene blue administration in septic shock: a clinical trial. Crit Care Med 23: 259–264.

Roberson ED, Sweatt JD (1996). Transient activation of cyclic AMP-dependent protein kinase during hippocampal long-term potentiation. J Biol Chem 271: 30436–30441.

Rodrigues JM, Pazin Filho A, Rodrigues AJ, Vicente WV, Evora PR (2007). Methylene blue for clinical anaphylaxis treatment: a case report. Sao Paulo Med J 125: 60–62.

Ryu H, Lee J, Impey S, Ratan RR, Ferrante RJ (2005). Antioxidants modulate mitochondrial PKA and increase CREB binding to D-loop DNA of the mitochondrial genome in neurons. Proc Natl Acad Sci U S A 102: 13915–13920.

Sayas CL, Ariaens A, Ponsioen B, Moolenaar WH (2006). GSK-3 is activated by the tyrosine kinase Pyk2 during LPA1-mediated neurite retraction. Mol Biol Cell 17: 1834–1844.

Schirmer RH, Adler H, Pickhardt M, Mandelkow E (2011). Lest we forget you – methylene blue. . . . Neurobiol Aging 32: 2325.e7–16.

Shackelford DB, Shaw RJ (2009). The LKB1–AMPK pathway: metabolism and growth control in tumour suppression. Nat Rev Cancer 9: 563–575.

Shin SM, Cho IJ, Kim SG (2009). Resveratrol protects mitochondria against oxidative stress through AMP-activated protein kinase-mediated glycogen synthase kinase-3beta inhibition downstream of poly(ADP-ribose)polymerase-LKB1 pathway. Mol Pharmacol 76: 884–895.

Suematsu N, Tsutsui H, Wen J, Kang D, Ikeuchi M, Ide T *et al*. (2003). Oxidative stress mediates tumor necrosis factor-alpha-induced mitochondrial DNA damage and dysfunction in cardiac myocytes. Circulation 107: 1418–1423.

Sun CK, Ng KT, Sun BS, Ho JW, Lee TK, Ng I *et al*. (2007). The significance of proline-rich tyrosine kinase2 (Pyk2) on hepatocellular carcinoma progression and recurrence. Br J Cancer 97: 50–57.

Tang L, Zhang Y, Jiang Y, Willard L, Ortiz E, Wark L *et al*. (2011). Dietary wolfberry ameliorates retinal structure abnormalities in db/db mice at the early stage of diabetes. Exp Biol Med (Maywood) 236: 1051–1063.

Tettamanti G, Malagoli D, Ottaviani E, de Eguileor M (2008). Oligomycin A and the IPLB-LdFB insect cell line: actin and mitochondrial responses. Cell Biol Int 32: 287–292.

Visarius TM, Stucki JW, Lauterburg BH (1999). Inhibition and stimulation of long-chain fatty acid oxidation by chloroacetaldehyde and methylene blue in rats. J Pharmacol Exp Ther 289: 820–824.

Wen Y, Li W, Poteet EC, Xie L, Tan C, Yan LJ *et al*. (2011). Alternative mitochondrial electron transfer as a novel strategy for neuroprotection. J Biol Chem 286: 16504–16515.

Xie Z, Dong Y, Scholz R, Neumann D, Zou MH (2008a). Phosphorylation of LKB1 at serine 428 by protein kinase C-zeta is required for metformin-enhanced activation of the AMP-activated protein kinase in endothelial cells. Circulation 117: 952–962.

Xie Z, Zhang J, Wu J, Viollet B, Zou MH (2008b). Upregulation of mitochondrial uncoupling protein-2 by the AMP-activated protein kinase in endothelial cells attenuates oxidative stress in diabetes. Diabetes 57: 3222–3230.

Xu L, Xu J, Liu S, Yang Z (2013). Induction of apoptosis by antimycin A in differentiated PC12 cell line. J Appl Toxicol doi: 10.1002/jat.2890. Epub ahead of print.

Zorov DB, Filburn CR, Klotz LO, Zweier JL, Sollott SJ (2000). Reactive oxygen species (ROS)-induced ROS release: a new phenomenon accompanying induction of the mitochondrial permeability transition in cardiac myocytes. J Exp Med 192: 1001–1014.

Supporting information

Additional Supporting Information may be found in the online version of this article at the publisher's web-site:

http://dx.doi.org/10.1111/bph.12637

Figure S1 The effects of MB on kinases of interest in primary hepatocytes. Immunoblottings were done on the lysates of primary rat hepatocytes treated with 1 μM MB for the indicated times.

Figure S2 The effect of STO-609 on AMPK activation by MB. Immunoblottings were done on the lysates of HepG2 cells treated with 0.3–3 $\mu g \cdot mL^{-1}$ STO-609 for 30 min, and continuously incubated with 1 μM MB for 6 h.

Figure S3 Immunoblottings for PKA. (A) The effect of MB on total or phosphorylated PKA levels. HepG2 cells were treated with 0.1 or 1 μM MB for 1 h, and were continuously incubated with 10 μM AA for 12 h, followed by exposure to 5 μM iron for 1 h. Immunoblottings were done on the cell lysates. Equal protein loading was verified by actin immunoblotting. For IP experiment, PKA immunoprecipitates (IP) were immunoblotted (IB) with anti-phosphorylated threonine antibody or anti-PKA antibody. (B) PKA levels in the liver. MB was orally administered to mice ($n = 4$) at a dose of 3 $mg \cdot kg^{-1} \cdot day^{-1}$ for 3 consecutive days. At 6 h after the last dose, mice were injected with a single dose of CCl_4 (i.p., 0.5 $mL \cdot kg^{-1}$ body wt, 1:20 in corn oil) and were killed 48 h thereafter. Liver homogenates were subjected to immunoblottings. (C) PKA levels in mitochondrial and cytoplasmic fractions. HepG2 cells were treated with 1 μM MB for the indicated times. Mitochondrial and cytoplasmic fractions were prepared as described in supplementary methods. Equal protein loading was verified by immunoblottings for VDAC (for mitochondria) or actin (for cytoplasm).

Figure S4 The effects of MB on LKB1 and AMPK phosphorylation. (A) Immunoblottings for phosphorylated LKB1 and AMPK in HepG2 cells. Cells were treated as described in Supporting Information Figure S3A. (B) Immunoblottings for phosphorylated LKB1 and AMPK in mouse liver. MB was orally administered to mice as described in Supporting Information Figure S3B. Immunoblottings were done on the liver homogenates.

Figure S5 Anti-inflammatory effect of MB. (A) TNFα and IL1β contents in plasma. Data represent the mean ± SEM from four animals. Statistical significance of differences between treatment and either the vehicle-treated group (**$P < 0.01$) or mice treated with CCl_4 ($^{\#}P < 0.05$, $^{\#\#}P < 0.01$) was determined. (B) Immunoblottings for iNOS and COX-2. Immunoblottings were done on the liver homogenates of mice treated as described in Supporting Information Figure 3B.